



OPEN

Early detection of feline chronic kidney disease via 3-hydroxykynurenone and machine learning

Ellen Vanden Broecke^{1,2}, Laurens Van Mulders^{1,2}, Ellen De Paepe¹, Dominique Paepe², Sylvie Daminet² & Lynn Vanhaecke^{1,3}✉

Feline chronic kidney disease (CKD) is one of the most frequently encountered diseases in veterinary practice, and the leading cause of mortality in cats over five years of age. While diagnosing advanced CKD is straightforward, current routine tests fail to diagnose early CKD. Therefore, this study aimed to identify early metabolic biomarkers. First, cats were retrospectively divided into two populations to conduct a case-control study, comparing the urinary and serum metabolome of healthy ($n=61$) and CKD IRIS stage 2 cats (CKD2, $n=63$). Subsequently, longitudinal validation was conducted in an independent population comprising healthy cats that remained healthy ($n=26$) and cats that developed CKD2 ($n=22$) within one year. Univariate, multivariate, and machine learning-based (ML) approaches were compared. The serum-to-urine ratio of 3-hydroxykynurenone was identified as a single biomarker candidate, yielding a high AUC (0.844) and accuracy (0.804), while linear support vector machine-based modelling employing metabolites and clinical parameters enhanced AUC (0.929) and accuracy (0.862) six months before traditional diagnosis. Furthermore, analysis of variable importance indicated consistent key serum metabolites, namely creatinine, SDMA, 2-hydroxyethanesulfonate, and aconitic acid. By enabling accurate diagnosis at least six months earlier, the highlighted metabolites may pave the way for improved diagnostics, ultimately contributing to timely disease management.

Keywords Diagnostic panel, Renal disease, Targeted metabolomics, Kynurenines, Machine learning algorithms, Multivariate models

Abbreviations

ACN	Acetonitrile
AUC	Area under the curve
BCS	Body condition score
CI	95% Confidence interval
CKD	Chronic kidney disease
CKD1	Chronic kidney disease IRIS stage 1
CKD2	Chronic kidney disease IRIS stage 2
CV	Coefficient of variation
FDR	False discovery rate
GFR	Glomerular filtration rate
GLM	Generalized linear model
HRMS	High-resolution mass spectrometry
IRIS	International renal interest society
ISTD	Internal standard
LASSO	Least absolute shrinkage and selection operator

¹Faculty of Veterinary Medicine, Department of Translational Physiology, Infectiology and Public Health, Laboratory of Integrative Metabolomics (LIMET), Ghent University, Salisburylaan 133, B-9820 Merelbeke, Belgium. ²Faculty of Veterinary Medicine, Small Animal Department, Ghent University, Salisburylaan 133, B-9820 Merelbeke, Belgium.

³School of Biological Sciences, Queen's University Belfast, Institute for Global Food Security, Chlorine Gardens 19, Belfast, Northern Ireland BT9-5DL, UK. ✉email: Lynn.Vanhaecke@Ugent.be

LIMMA	Linear model for microarray data
MeOH	Methanol
<i>m/z</i>	Mass-to-charge ratio
PCA-X	Principal component analysis
Q-orbitrap	Quadrupole orbitrap
QC	Quality control
RF	Random forest
ROC	Receiver operating characteristic curve
Rt	Retention time
S	Serum
S/U	Serum-to-urine ratio
SBP	Systolic blood pressure
SDMA	Symmetric dimethylarginine
SVM	Support vector machine
U	Urine
U/S	Urine-to-serum ratio
UHPLC	Ultra-high performance liquid chromatography
UPC	Urinary protein-creatinine ratio
UPW	Ultrapure water
USG	Urinary specific gravity

Feline chronic kidney disease (CKD) poses a significant challenge in veterinary practice, with a considerable impact on mortality rates among cats over five years of age^{1,2}. Despite its high prevalence, veterinarians face significant challenges in diagnosing early or non-azotemic CKD³. However, early detection and therefore timely therapeutic interventions are generally more effective when initiated in the early stages of the disease, improving prognosis and lifespan^{4,5}.

While the measurement of glomerular filtration rate (GFR) is considered the most sensitive parameter for assessing renal function, its routine analysis is not practical in everyday veterinary practice due to its labour-intensive and time-consuming nature^{5–7}. As a result, CKD is typically diagnosed by evaluating a combination of medical history, clinical findings, routine blood tests to assess the presence of azotemia, combined with urinalysis to identify poorly concentrated urine^{5,8}. However, these methods all come with significant shortcomings, including inadequate sensitivity and specificity^{9–11}. As a result, kidney damage often goes undetected until approximately 75% of nephrons have been damaged^{5,12}. Although the knowledge on renal biomarkers in feline CKD has progressed substantially over the last five years¹³, the available biomarkers are not thoroughly validated to accurately detect renal function deterioration at an early stage.

By focusing on the comprehensive analysis of small molecules present in cells, tissues, and body fluids, collectively known as the metabolome, metabolomics can offer a highly accurate representation of an organism's pathophysiological status. Although this technology holds great promise, few studies have been conducted in the context of feline CKD. Existing studies, such as Rivera-Velez and Villarino's urinary metabolomics analysis in healthy cats¹⁴, and the metabolomic profiling of serum in feline CKD by Nealon et al.¹⁵ underscore the potential of this approach in understanding feline physiology and diseases. However, by primarily focusing on one-off case-control comparisons, longitudinal assessments of potential biomarkers for early diagnosis are lacking, highlighting a significant research gap.

Recognizing the urgent need for more comprehensive approaches to identify reliable early biomarkers for feline CKD, this study aims to explore the potential of metabolomics in addressing the deficits of current diagnostic tools. By employing a targeted or "hypothesis-driven" approach, measuring ions from defined metabolites, this study seeks to unravel the comprehensive metabolic profile of feline CKD and validate predictive performance of potential biomarkers in an independent longitudinal cohort.

Results

Population demographics

The baseline study population consisted of 61 healthy cats, and 63 cats with CKD IRIS stage 2 (CKD2), classified according to the International Renal Interest Society (IRIS) guidelines^{16,17}. The longitudinal population of initially healthy cats counted 26 cats remaining healthy and 22 cats developing CKD2. Demographics of both study groups are presented in Table 1, with data from three timepoints for the longitudinal population (i.e. at the point of traditional CKD diagnosis (T_0), six (T_6) and twelve months (T_{12}) prior to diagnosis). Breeds for the baseline/longitudinal population included British Longhair (n = 1/1), British Shorthair (n = 18/5), Burmese (n = 1/0), Domestic Longhair (n = 1/0), Domestic Shorthair (n = 95/36), LaPerm (n = 0/1), Main Coone (n = 2/2), Oriental Shorthair (n = 1/0), Persian (n = 0/1), Ragdoll (n = 3/1), Russian Blue (n = 1/0) and Siamese (n = 1/1), respectively. Pairwise comparisons did not reveal a significant difference in age, gender, albumin, potassium, urinary protein-creatinine ratio (UPC) and urinary culture (i.e., positive or negative) between healthy cats and cats developing or having CKD2. The body condition score (BCS) and muscle condition score (MCS) were significantly lower in the baseline CKD2 population than in the healthy baseline cats, but not in the longitudinal follow-up study. For the systolic blood pressure (SBP), only cats developing CKD2 had a significant higher SBP at T_{-12} (42% with an SBP > 160 mmHg) compared to cats remaining healthy at T_{-12} (24% with an SBP > 160 mmHg), but this did not persist through the follow-up (CKD2: 29% and 38% with an SBP > 160 mmHg at T_6 and T_0 ; healthy: 30% and 19% with an SBP > 160 mmHg at T_6 and T_0 , respectively). In the baseline population, these numbers were not significantly different, with 36% of CKD cats and 29% of healthy cats demonstrating a SBP > 160 mmHg. As expected, creatinine, symmetric dimethylarginine (SDMA), urea and urinary specific

Baseline population					
Number	Healthy	CKD2	P-value	RI	
	N=61	N=63			
Sex (M, MC, F, FS)	1, 27, 3, 30	1, 28, 2, 32	0.9999 ^c		
Age (years)	12.6 (2.5)	14.9 (5.3)	0.0756 ^b		
BCS (/9)	5 (2)	4 (2)	0.0007 ^b		
MCS (/4)	2 (1)	2 (1)	0.0013 ^b		
SBP (mmHg)	151 (23)	153 (23)	0.6707 ^a		
Creatinine ($\mu\text{mol/L}$)	119 (26)	198 (29)	<0.0001 ^b	71–164	
SDMA ($\mu\text{g/dL}$)	9.3 (3.2)	14.6 (4.4)	<0.0001 ^b	8.0–14.0	
Urea (mmol/L)	9.1 (2.5)	14.4 (3.9)	<0.0001 ^b	5.8–12.0	
Albumin (g/L)	39 (4)	39 (6)	0.7966 ^b	29–44	
Total calcium (mmol/L)	2.4 (0.2)	2.5 (0.2)	<0.0001 ^b	2.3–2.8	
Phosphate (mmol/L)	1.3 (0.2)	1.4 (0.2)	0.0010 ^a	1.0–2.4	
Potassium (mmol/L)	4.4 (0.4)	4.5 (0.5)	0.4223 ^a	3.8–5.3	
USG	1.047 (0.010)	1.021 (0.014)	<0.0001 ^b	≥ 1.035	
UPC	0.16 (0.11)	0.18 (0.18)	0.6104 ^b	<0.40	
Pos urinary culture	N=1	N=6	0.1134 ^d		
Longitudinal population					
Number	Healthy \rightarrow Healthy	Healthy \rightarrow CKD2	P-value	RI	
	N=26	N=22			
Sex (MC, FS)	12, 14	8, 14	0.6953 ^c		
Age at inclusion (years)	12.0 (1.4)	13.4 (3.0)	0.0943 ^a		
BCS (/9)	T ₋₁₂ 5 (1)	5 (2.5)	0.2438 ^b		
	T ₋₆ 5 (1.25)	4.5 (2)	0.2725 ^b		
	T ₀ 5 (2)	4 (1)	0.1673 ^b		
MCS (/4)	T ₋₁₂ 2 (0)	2 (1)	0.1982 ^b		
	T ₋₆ 2 (0)	2 (0)	0.5754 ^b		
	T ₀ 2 (0)	2 (1)	0.8033 ^b		
SBP (mmHg)	T ₋₁₂ 150 (25)	167 (19)	0.0256 ^a		
	T ₋₆ 150 (35)	150 (20)	0.5426 ^b		
	T ₀ 146 (19)	154 (22)	0.2187 ^a		
Creatinine ($\mu\text{mol/L}$)	T ₋₁₂ 122 (21)	131 (18)	0.1064 ^a	71–164	
	T ₋₆ 115 (15)	138 (15)	<0.0001 ^a		
	T ₀ 126 (15)	182 (21)	<0.0001 ^b		
SDMA ($\mu\text{g/dL}$)	T ₋₁₂ 9.5 (2.3)	11.2 (2.4)	0.0450 ^a	8.0–14.0	
	T ₋₆ 8.8 (2.2)	11.7 (2.8)	0.0791 ^a		
	T ₀ 7.4 (3.3)	12.8 (4.9)	0.0005 ^b		
Urea (mmol/L)	T ₋₁₂ 8.7 (1.7)	10.1 (3.1)	0.1053 ^b	5.8–12.0	
	T ₋₆ 8.6 (1.1)	11.6 (2.3)	0.0037 ^a		
	T ₀ 8.3 (1.5)	11.5 (4.8)	<0.0001 ^b		
Albumin (g/L)	T ₋₁₂ 38 (3)	40 (5)	0.4299 ^a	29–44	
	T ₋₆ 36 (3)	38 (4)	0.2086 ^a		
	T ₀ 36 (4)	37 (3)	0.3679 ^a		
Total calcium (mmol/L)	T ₋₁₂ 2.4 (0.2)	2.4 (0.2)	0.8657 ^b	2.3–2.8	
	T ₋₆ 2.4 (0.1)	2.4 (0.1)	0.7229 ^a		
	T ₀ 2.4 (0.1)	2.5 (0.2)	0.1355 ^b		
Phosphate (mmol/L)	T ₋₁₂ 1.3 (0.3)	1.3 (0.2)	0.5948 ^a	1.0–2.4	
	T ₋₆ 1.3 (0.3)	1.4 (0.2)	0.5159 ^a		
	T ₀ 1.3 (0.3)	1.4 (0.2)	0.2804 ^a		
Potassium (mmol/L)	T ₋₁₂ 4.3 (0.4)	4.4 (0.3)	0.5574 ^a	3.8–5.3	
	T ₋₆ 4.4 (0.4)	4.5 (0.3)	0.4987 ^a		
	T ₀ 4.3 (0.4)	4.4 (0.6)	0.8209 ^a		
USG	T ₋₁₂ 1.045 (0.008)	1.037 (0.011)	0.0132 ^b	≥ 1.035	
	T ₋₆ 1.048 (0.007)	1.031 (0.009)	<0.0001 ^a		
	T ₀ 1.045 (0.009)	1.019 (0.010)	<0.0001 ^b		

Continued

Longitudinal population					
Number		Healthy → Healthy	Healthy → CKD2	P-value	RI
	N = 26	N = 22			
UPC	T ₋₁₂	0.14 (0.06)	0.17 (0.06)	0.307 ^b	< 0.40
	T ₋₆	0.15 (0.05)	0.16 (0.11)	0.610 ^b	
	T ₀	0.14 (0.05)	0.14 (0.01)	0.520 ^b	
Pos urinary culture	T ₋₁₂ N = 2	N = 2		0.6080 ^d	
	T ₋₆ N = 1	N = 1		0.9999 ^d	
	T ₀ N = 0	N = 1		0.4565 ^d	

Table 1. Demographic and clinical characteristics in the baseline and longitudinal populations, on T₋₁₂, T₋₆ and T₀. F female, FS female spayed, M male, MC male castrated, RI reference interval. Results are expressed as the mean (standard deviation) or the median (interquartile range), as appropriate. P-values resulting from pairwise comparisons are reported as well. Either a Welch two-sample t test (parametric data^a) or Wilcoxon rank-sum test (non-parametric data, ^b) was employed for continuous variables. For gender, the Chi-squared test (^c) was applied. For urinary culture, the Fisher's Exact test (^d) was employed.

gravity (USG) were significantly different in the baseline population. While creatine and urea also significantly increased in cats developing CKD starting from T₋₆, SDMA fluctuated and only showed a significant difference at T₀ and T₋₁₂. Finally, phosphate and total calcium were significantly different in the baseline population but not in the longitudinal population.

Metabolic alterations in CKD2 compared to healthy cats

Targeted metabolic profiling generated 80 serum (S) and 64 urinary (U) metabolites. A total of 61 metabolites were found to be common to both matrices, thus enabling the calculation of ratios between them (i.e. serum-over-urine (S/U) and urine-over serum (U/S)). Based on CKD-associated pathways, ratios of 45 serum and 36 urinary metabolites were calculated. This resulted in a total of 413 metabolites and metabolites ratios across both matrices and ratios of matrices (Supplementary Table S1). Univariate pairwise statistics were applied as a first exploratory step on both study groups to detect significantly altered metabolites and metabolite ratios (Supplementary Tables S1 until S3, Fig. 1). For the longitudinal population, no significant differences were detected at T₋₁₂. For T₋₆, a total of 92 significantly different metabolites and metabolites ratios were detected, with the most significant alterations in urine and ratios of matrices. This was similar for the comparison of CKD2 and healthy cats at T₀ of the longitudinal population and the baseline population, with a total of 261 significant differences (Supplementary Tables S1 until S3, Fig. 1a). From these data, S/U 3-hydroxykynurenine could be assigned a promising biomarker for early detection, as it remained stable (non-significantly different) in the healthy group but showed a gradual increase in cats developing CKD2 over the follow-up period (Fig. 1c). Moreover, the 3-hydroxykynurenine S/U ratio proved to be even more significant (Adj. P = 0.002) at T₋₆ compared to 3-hydroxykynurenine concentrations in serum (Adj. P = 0.526) or urine (Adj. P = 0.006) (Supplementary Fig. S1). The proposed predictive capacity of this metabolite in S/U was additionally validated through univariate logistic regression, as illustrated in Table 2.

Although some degree of overlap is evident, multivariate exploratory principal component analyses (PCA-X) demonstrated a certain clustering of the two groups in both matrices at T₀, and even at T₋₆ (Fig. 1b). These findings support our hypothesis that potential biomarkers for early detection could be uncovered from our a priori selected panel of endogenous metabolites.

Predictive modelling for CKD2

In order to assess the predictive performance of individual biomarkers and panels, several strategies for data analysis were evaluated. Univariate binary logistic regression was employed to evaluate the predictive capacity of single metabolites and metabolite ratios. To assess whether a combination of candidate biomarkers could enhance performance, multivariate statistics, including least absolute shrinkage and selection operator (LASSO) regression and linear model for microarray data (LIMMA) with subsequent generalized linear modelling (GLM), were utilized. Furthermore, machine learning (ML)-based modelling was employed to make predictions with the full dataset, through the use of random forest (RF) and support vector machine (SVM).

First of all, performance metrics (i.e., area under the curve (AUC), accuracy, sensitivity and specificity) were determined for each individual metabolite and metabolite ratio in both matrices and ratios of matrices using univariate binary logistic regression, of which the top 15 are presented in Tables 2 and 3, and Supplementary Table S4. To evaluate their predictive performance prior to the point of traditional diagnosis, metabolites and metabolite ratios were sorted according to the highest AUC at T₋₆. The matrix ratio of S/U 3-hydroxykynurenine was confirmed as the best potential individual biomarker for early CKD, resulting in the highest performance at T₀, T₋₆, and T₋₁₂ (Table 2). It is notable that, despite suggestions that serum SDMA may serve as an early biomarker of CKD, it was only identified as the 14th most predictive individual metabolite at T₋₆, however it did emerge as the 4th best predictor at T₋₁₂ when sorted on AUC.

The top 15 metabolites are presented, sorted according to the highest AUC-value at T₋₆.

In a second step, the predictive capacity of biomarker panels were evaluated through multivariate statistics, using LASSO regression and LIMMA with subsequent GLM for feature selection. With the tuning parameter λ

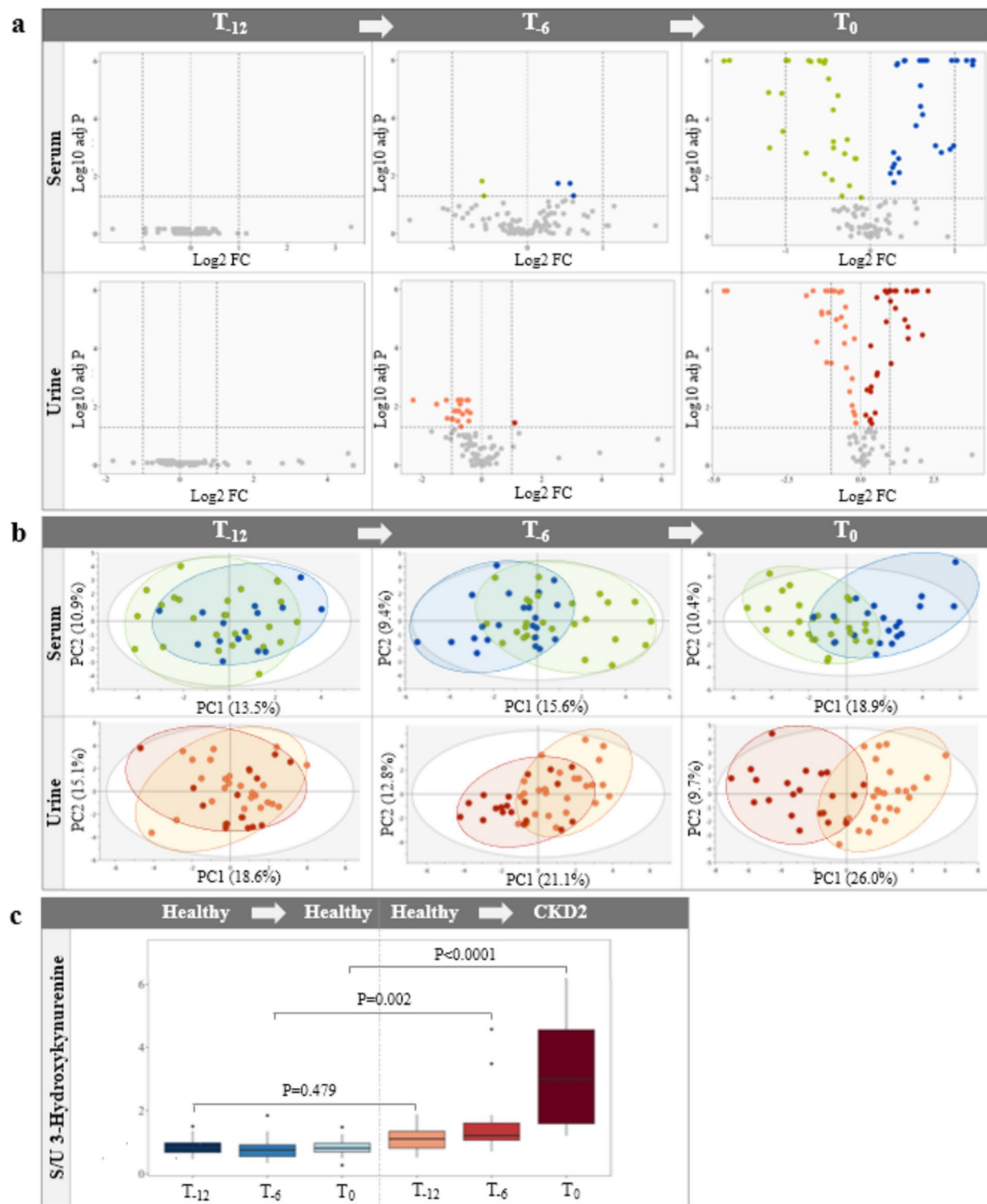


Fig. 1. Visualisation of changing serum and urinary metabolome in the longitudinal population on T₋₁₂, T₋₆ and T₀. (a) Volcano plots illustrating significantly decreased (green and orange) and increased (blue and red) metabolites and metabolite ratios in serum and urine, respectively. (b) PCA-X score plots of all targeted serum and urinary metabolites and metabolite ratios for healthy cats remaining healthy (green and orange, respectively) and developing CKD2 (blue and red, respectively). (c) Box plot representation of S/U 3-hydroxykynurenone in healthy cats remaining healthy (blue shades) and developing CKD2 (red shades). Significant differences (FDR (false discovery rate) corrected P-value < 0.05) in the CKD2 group could be observed from T₋₆ onwards.

Matrix	Metabolite	T ₀		T ₋₆		T ₋₁₂	
		AUC	CI	AUC	CI	AUC	CI
S/U	3-Hydroxykynurenine	0.990	0.973–1.000	0.844	0.729–0.959	0.692	0.507–0.878
U/S	3-Hydroxykynurenine	0.990	0.973–1.000	0.844	0.729–0.959	0.692	0.507–0.878
S/U	Isoleucine	0.834	0.700–0.969	0.842	0.714–0.970	0.613	0.402–0.824
S/U	Creatinine	0.931	0.853–1.000	0.840	0.720–0.961	0.772	0.628–0.916
U/S	Creatinine	0.931	0.853–1.000	0.840	0.720–0.961	0.772	0.628–0.916
S/U	Kynurenic acid	0.905	0.819–0.990	0.833	0.701–0.964	0.669	0.499–0.840
U/S	Kynurenic acid	0.905	0.819–0.990	0.833	0.701–0.964	0.669	0.499–0.840
U	3-Hydroxykynurenine	0.975	0.941–1.000	0.827	0.706–0.947	0.635	0.454–0.815
S	Tryptophan/5-hydroxyindole-3-acetic acid	0.901	0.816–0.987	0.813	0.686–0.939	0.685	0.514–0.856
U	Serotonin	0.871	0.768–0.974	0.796	0.663–0.929	0.605	0.406–0.804
U	Adenosine	0.913	0.818–1.000	0.794	0.659–0.930	0.699	0.532–0.866
U	Creatine/guanidinosuccinate	0.849	0.726–0.972	0.781	0.637–0.924	0.575	0.395–0.755
U	Creatinine/guanidinosuccinate	0.849	0.726–0.972	0.781	0.637–0.924	0.575	0.395–0.755
S	SDMA	0.904	0.821–0.986	0.778	0.642–0.914	0.715	0.553–0.878
S	Trimethylamine-N-oxide	0.808	0.676–0.939	0.777	0.638–0.916	0.500	0.315–0.685
		AUC	CI	AUC	CI	AUC	CI
S/U	3-Hydroxykynurenine	0.913	0.792–0.976	0.804	0.661–0.906	0.804	0.571–0.858
U/S	3-Hydroxykynurenine	0.870	0.737–0.951	0.783	0.636–0.891	0.783	0.519–0.819
S/U	Isoleucine	0.761	0.612–0.874	0.783	0.636–0.891	0.783	0.374–0.693
S/U	Creatinine	0.783	0.636–0.891	0.717	0.565–0.840	0.717	0.545–0.839
U/S	Creatinine	0.739	0.589–0.857	0.696	0.542–0.823	0.696	0.469–0.779
S/U	Kynurenic acid	0.652	0.498–0.786	0.652	0.498–0.786	0.652	0.421–0.737
U/S	Kynurenic acid	0.609	0.454–0.749	0.587	0.432–0.730	0.587	0.397–0.715
U	3-Hydroxykynurenine	0.787	0.643–0.893	0.674	0.520–0.805	0.674	0.480–0.784
S	Tryptophan/5-hydroxyindole-3-acetic acid	0.638	0.485–0.773	0.583	0.432–0.724	0.583	0.374–0.693
U	Serotonin	0.681	0.529–0.809	0.587	0.432–0.730	0.587	0.256–0.567
U	Adenosine	0.872	0.743–0.952	0.739	0.589–0.857	0.739	0.554–0.843
U	Creatine/guanidinosuccinate	0.574	0.422–0.717	0.565	0.411–0.711	0.565	0.364–0.680
U	Creatinine/guanidinosuccinate	0.574	0.422–0.717	0.565	0.411–0.711	0.565	0.364–0.680
S	SDMA	0.761	0.612–0.874	0.674	0.520–0.805	0.674	0.545–0.839
S	Trimethylamine-N-oxide	0.587	0.432–0.730	0.630	0.475–0.768	0.630	0.307–0.626

Table 2. Performance metrics (i.e. AUC and accuracy) of individual metabolites and metabolite ratios for the classification of healthy and CKD2 in the longitudinal population.

set at 0.003 for LASSO, a predictive model incorporating 21 serum metabolites achieved the highest performance at T₀, T₋₆ and T₋₁₂ (Table 4).

More specifically, the logistic regression function to estimate the probability of developing CKD2 using the serum metabolites selected by LASSO was defined as

$$P(\text{CKD2}) = \frac{1}{1 + \exp(-z)}$$

with $z = 0.055 + 6.424 \times \text{creatinine} + 2.706 \times \text{SDMA} + 2.672 \times 2\text{-hydroxyethanesulfonate} + 2.255 \times 3\text{-hydroxykynurenine} - 1.828 \times \text{tryptophan} + 1.505 \times \text{dimethylglycine} - 0.958 \times \text{serotonin} + 0.923 \times \text{carnosine} + 0.764 \times \text{indole-3-acetic acid} - 0.663 \times \text{uric acid} + 0.578 \times \text{creatine} + 0.509 \times \text{aconitic acid} - 0.485 \times \text{guanidinoacetate} + 0.249 \times \text{citramalic acid} - 0.186 \times \text{ADMA} - 0.173 \times \text{glutamine} + 0.089 \times \text{indoxy sulphate} - 0.085 \times \text{xanthine} + 0.075 \times \text{p-cresol} + 0.047 \times \text{2-aminoisobutyric acid} + 0.007 \times \text{picolinic acid}$.

As an alternative feature selection method, a combination of LIMMA with multivariate GLM modelling was applied to train models with the two to ten highest ranked metabolites and metabolite ratios (Supplementary Tables S5 and S6). The highest AUC and accuracy were once again obtained using serum metabolites (n=8) (Table 4). The predictive model resulting from LIMMA with GLM was defined by the following logistic function using serum metabolites:

Matrix	Metabolite	Estimate	SE	OR	CI	P-value
S/U	3-Hydroxykynurenine	3.563	0.738	35.270	8.299–149.893	<0.0001
U/S	3-Hydroxykynurenine	-3.668	0.756	0.026	0.006–0.112	<0.0001
S/U	Isoleucine	0.720	0.333	2.054	1.069–3.946	0.0308
S/U	Creatinine	-0.356	0.320	40.122	8.520–188.994	<0.0001
U/S	Creatinine	3.692	0.791	0.018	0.003–0.093	<0.0001
S/U	Kynurenic acid	-4.043	0.852	4.036	1.243–13.107	0.0202
U/S	Kynurenic acid	1.395	0.601	0.285	0.119–0.681	0.0048
U	3-Hydroxykynurenine	-1.255	0.445	0.144	0.036–0.571	0.0058
S	Tryptophan/5-hydroxyindole-3-acetic acid	-1.940	0.703	0.093	0.037–0.237	<0.0001
U	Serotonin	0.228	0.312	0.225	0.109–0.463	0.0001
U	Adenosine	-0.461	0.393	0.120	0.045–0.322	<0.0001
U	Creatine/guanidinosuccinate	-2.372	0.477	0.172	0.075–0.396	<0.0001
U	Creatinine/guanidinosuccinate	-0.534	0.372	0.172	0.075–0.396	<0.0001
S	SDMA	0.810	0.150	2.248	1.674–3.020	<0.0001
S	Trimethylamine-N-oxide	1.285	0.415	3.614	1.601–8.155	0.0020

Table 3. Metrics of logistic regression using a binomial GLM for the top 15 metabolites and metabolite ratios for the classification of healthy and CKD2 in the baseline population. Statistical significance was evaluated using the Wald test. SE standard error, OR odds ratio.

	N	Timepoint	AUC	CI	Accuracy	CI
LASSO						
Serum	21	T ₀	0.973	0.937–1.000	0.894	0.769–0.965
		T ₋₆	0.816	0.693–0.940	0.750	0.604–0.864
		T ₋₁₂	0.736	0.584–0.888	0.659	0.494–0.799
Urine	11	T ₀	0.489	0.319–0.660	0.468	0.321–0.619
		T ₋₆	0.367	0.198–0.537	0.370	0.232–0.525
		T ₋₁₂	0.370	0.194–0.547	0.429	0.277–0.590
Combined	6	T ₀	0.874	0.773–0.975	0.783	0.636–0.891
		T ₋₆	0.652	0.489–0.815	0.630	0.475–0.768
		T ₋₁₂	0.638	0.456–0.821	0.610	0.445–0.758
LIMMA						
Serum	8	T ₀	0.974	0.940–1.000	0.872	0.743–0.952
		T ₋₆	0.823	0.702–0.944	0.771	0.627–0.880
		T ₋₁₂	0.746	0.596–0.896	0.659	0.494–0.799
Urine	12	T ₀	0.618	0.454–0.782	0.617	0.464–0.755
		T ₋₆	0.519	0.345–0.693	0.500	0.349–0.651
		T ₋₁₂	0.462	0.276–0.647	0.429	0.277–0.590
Combined	12	T ₀	0.926	0.848–1.000	0.870	0.737–0.951
		T ₋₆	0.778	0.645–0.911	0.674	0.520–0.805
		T ₋₁₂	0.726	0.567–0.884	0.659	0.494–0.799

Table 4. Predictive performance of models using LASSO regression and LIMMA with subsequent GLM in serum, urine and both matrices combined. N = number of metabolites included in the biomarker panel. AUC and accuracy were evaluated at T₋₁₂, T₋₆ and T₀. For LIMMA, only the models obtaining the highest performance at T₋₆ are presented for each matrix.

– 0.267 – 25.493 × isocitrate + 21.9967 × citric acid + 8.705 × creatinine + 6.602 × SDMA + 6.102 × aconitic acid + 2.110 × kynurenic acid + 1.991 × 1-methylhistidine + 1.189 × 2-hydroxyethanesulfonate.

Thirdly, ML techniques (i.e., RF and SVM) revealed similar results to LASSO and LIMMA, more specifically, the best predictive capacity was obtained using metabolites and metabolite ratios from the serum matrix (Table 5). For these serum models, the optimal number of variables (mtry) at each split point of the tree when using RF was found to be 10. For SVM, the C-value was set at 0.6 and 2.0 for the linear and radial model, respectively.

In order to identify which statistical or ML-based approach could best predict CKD2, AUC and accuracy values were compared at T₋₆. For the univariate statistics, 3-hydroxykynurenine was selected for comparison since this metabolites yielded the highest predictive performance as an individual candidate biomarker. For LASSO and LIMMA, the serum biomarkers panels (n = 21 and n = 8, respectively) were chosen, and for RF and SVM, models

	Timepoint	AUC	CI	Accuracy	CI
RF					
Serum	T ₀	0.974	0.937–1.000	0.915	0.796–0.976
	T ₋₆	0.818	0.698–0.938	0.771	0.627–0.880
	T ₋₁₂	0.687	0.519–0.855	0.634	0.469–0.779
Urine	T ₀	0.712	0.561–0.863	0.660	0.507–0.791
	T ₋₆	0.544	0.370–0.718	0.478	0.329–0.631
	T ₋₁₂	0.496	0.308–0.684	0.429	0.277–0.590
Combined	T ₀	0.950	0.897–1.000	0.848	0.711–0.937
	T ₋₆	0.757	0.612–0.902	0.761	0.612–0.874
	T ₋₁₂	0.623	0.445–0.801	0.585	0.421–0.737
SVM linear					
Serum	T ₀	0.978	0.946–1.000	0.915	0.796–0.976
	T ₋₆	0.864	0.756–0.972	0.771	0.627–0.880
	T ₋₁₂	0.756	0.607–0.906	0.683	0.519–0.819
Urine	T ₀	0.922	0.843–1.000	0.766	0.620–0.877
	T ₋₆	0.562	0.382–0.741	0.500	0.349–0.651
	T ₋₁₂	0.519	0.327–0.711	0.357	0.216–0.520
Combined	T ₀	0.964	0.919–1.000	0.891	0.764–0.964
	T ₋₆	0.783	0.648–0.917	0.674	0.520–0.805
	T ₋₁₂	0.662	0.481–0.842	0.512	0.351–0.671
SVM radial					
Serum	T ₀	0.989	0.970–1.000	0.915	0.796–0.976
	T ₋₆	0.876	0.774–0.977	0.771	0.627–0.880
	T ₋₁₂	0.751	0.593–0.909	0.707	0.545–0.839
Urine	T ₀	0.820	0.696–0.944	0.681	0.529–0.809
	T ₋₆	0.521	0.345–0.697	0.522	0.369–0.671
	T ₋₁₂	0.585	0.401–0.770	0.500	0.342–0.658
Combined	T ₀	0.975	0.942–1.000	0.891	0.764–0.964
	T ₋₆	0.802	0.668–0.936	0.674	0.520–0.805
	T ₋₁₂	0.710	0.549–0.871	0.585	0.421–0.737

Table 5. Predictive performance of ML-based models, including RF and SVM, both linear and radial in serum, urine and both matrices combined. AUC and accuracy were evaluated at T₋₁₂, T₋₆ and T₀.

utilising all serum metabolites were employed for comparison. While 3-hydroxykynurenone demonstrated the highest accuracy (0.804), the confidence intervals exhibited substantial overlap for all approaches (Fig. 2). A similar pattern could be observed for the AUC values, with the radial SVM model performing best (0.876) (Fig. 3). Identical accuracy values were observed for LIMMA, RF and SVM (0.771). This was attributed to an identical number of accurate predictions for healthy and CKD combined (Supplementary Fig. S2). However, the number of cases and controls with correct predictions varied between models, as well as which cats were correctly classified. Additionally, sensitivity and specificity were also calculated as presented in Supplementary Tables S4 and S7, demonstrating a reasonable sensitivity and specificity at T₋₆ for S/U 3-hydroxykynurenone (0.750 and 0.846, respectively), while multivariate and ML-based serum models demonstrated slightly higher sensitivity (i.e., between 0.773–0.864), and lower specificity (i.e., between 0.692–0.731).

A thorough analysis of variable importance was performed on the models built with the baseline population, indicating consistent identification of key metabolites in the multivariate and ML-based models. The relative variable importance of the selected metabolites is presented in Fig. 3, containing all included variables for the LASSO and LIMMA models, and the top 15 variables for RF and SVM. No difference was observed in variable importance between the linear and radial SVM. Overall, creatinine, SDMA, 2-hydroxyethanesulfonate and aconitic acid consistently emerged as important variables across all multivariate and ML-based models. Furthermore, a comparison of the LIMMA, RF and SVM models revealed that the first eight metabolites are similar, although the order differs. The same analysis was conducted for the urinary and combined models, and the results are presented in Supplementary Fig. S4 and S5, together with the corresponding predictive functions.

Predictive modelling for CKD2 using metabolites and clinical parameters

We also evaluated whether the clinical parameters as described in Table 1 could enhance the longitudinal predictive capacity. These additional variables included age, SBP, BCS, MCS, urea, albumin, total calcium, phosphate, potassium, UPC, USG and urinary culture (i.e. positive or negative), and were collectively incorporated alongside the metabolite data for model development. In accordance with the findings of our preceding analysis, models incorporating serum metabolites once again exhibited the highest degree of predictive

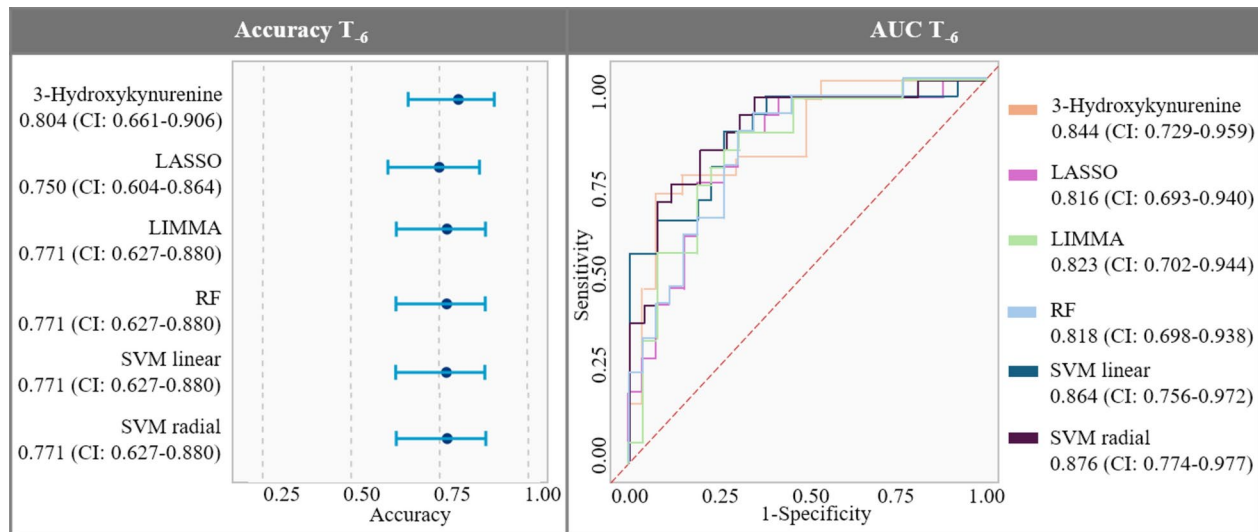


Fig. 2. Accuracy dot plots and ROC curves for predictions on T₆. The corresponding accuracy and AUC values with 95% CI are reported for S/U 3-hydroxykynurenine, both multivariate serum models (i.e. LASSO regression and LIMMA with subsequent GLM) and ML-based serum models (i.e. RF and SVM).

capacity, a phenomenon that persisted even when clinical parameters were included. While urea was included in the LASSO ($n=5$, $\lambda=0.1$) and LIMMA model ($n=12$) following the automated feature selection procedure, no other clinical parameters were selected in the model building phase. Furthermore, urea also positioned in the top 15 variables based on analysis of variable importance for the RF (mtry = 6) and SVM (linear: C = 0.6, radial: C = 4.0) models. By adding the clinical parameters to model building phase, both AUC and accuracy could be enhanced for all models at T₆ and T₁₂ (Table 6), compared to the models employing solely metabolites from the targeted panel (Tables 4 and 5). Besides urea, other variables that showed high importance in all models included creatinine, SDMA, 2-hydroxyethanesulfonate and aconitic acid (Fig. 4), similar as the models built without clinical parameters.

To predict CKD2 development using the combined serum metabolites and clinical parameters selected by LASSO, the following logistic regression function can be applied:

$$P(\text{CKD2}) = \frac{1}{1 + \exp(-z)}$$

with $z = -0.488 + 1.359 \times \text{creatinine} + 1.087 \times 2\text{-hydroxyethanesulfonate} + 0.418 \times \text{SDMA} + 0.027 \times \text{urea} + 0.001 \times \text{aconitic acid}$.

For LIMMA with GLM modelling, z equals:

$-37.405 + 136.937 \times \text{isocitrate} - 123.796 \times \text{citric acid} + 50.994 \times \text{creatinine} + 35.149 \times \text{SDMA} + 14.537 \times \text{allantoin} - 13.129 \times \text{ADMA} - 8.883 \times 5\text{-hydroxyindoleacetic acid} - 8.831 \times \text{kynurenic acid} + 6.352 \times 2\text{-hydroxyethanesulfonate} + 3.970 \times 1\text{-methylhistidine} + 3.097 \times \text{urea} - 3.011 \times \text{aconitic acid}$.

Discussion

This study highlights the potential of metabolomics to overcome the diagnostic challenges of early feline CKD. Using a metabolic profiling approach, we identified several key metabolites and metabolite ratios that allow earlier detection of CKD, up to six months before traditional diagnosis. Multi-biomarker panels included creatinine, 2-hydroxyethanesulfonate, 1-methylhistidine, aconitic acid and various kynurene-related compounds, resulting from multivariate and ML-based modelling. In addition, S/U 3-hydroxykynurenine showed potential as an individual biomarker.

3-Hydroxykynurenine exhibited the highest predictive performance in the univariate regression analysis. As the principal route of tryptophan degradation, 3-hydroxykynurenine is metabolised via the kynurene pathway^{18,19}. Since the kidneys play a crucial role in tryptophan metabolism²⁰, renal pathologies can greatly disturb this pathway. As kynurenes are eliminated via urinary excretion²¹, a decreased GFR can lead to increased plasma and tissue concentrations of tryptophan metabolites, as demonstrated in several human and rodent studies on CKD²²⁻²⁵. More specifically, the study of Pawlak et al. (2009) demonstrated a 184–306% increase in human patients with CKD.²² Furthermore, the accumulation of kynurenes may result in oxidative cell damage, dysregulation of calcium homeostasis and mitochondrial dysfunction in cells, leading to severe metabolic disorders and inflammatory processes^{19,26-29}.

Although of great importance in all models, 2-hydroxyethanesulfonate or isethionic acid has only been reported to a limited extent in the context of CKD. It is an alkanesulfonate that is involved in (hypo)taurine

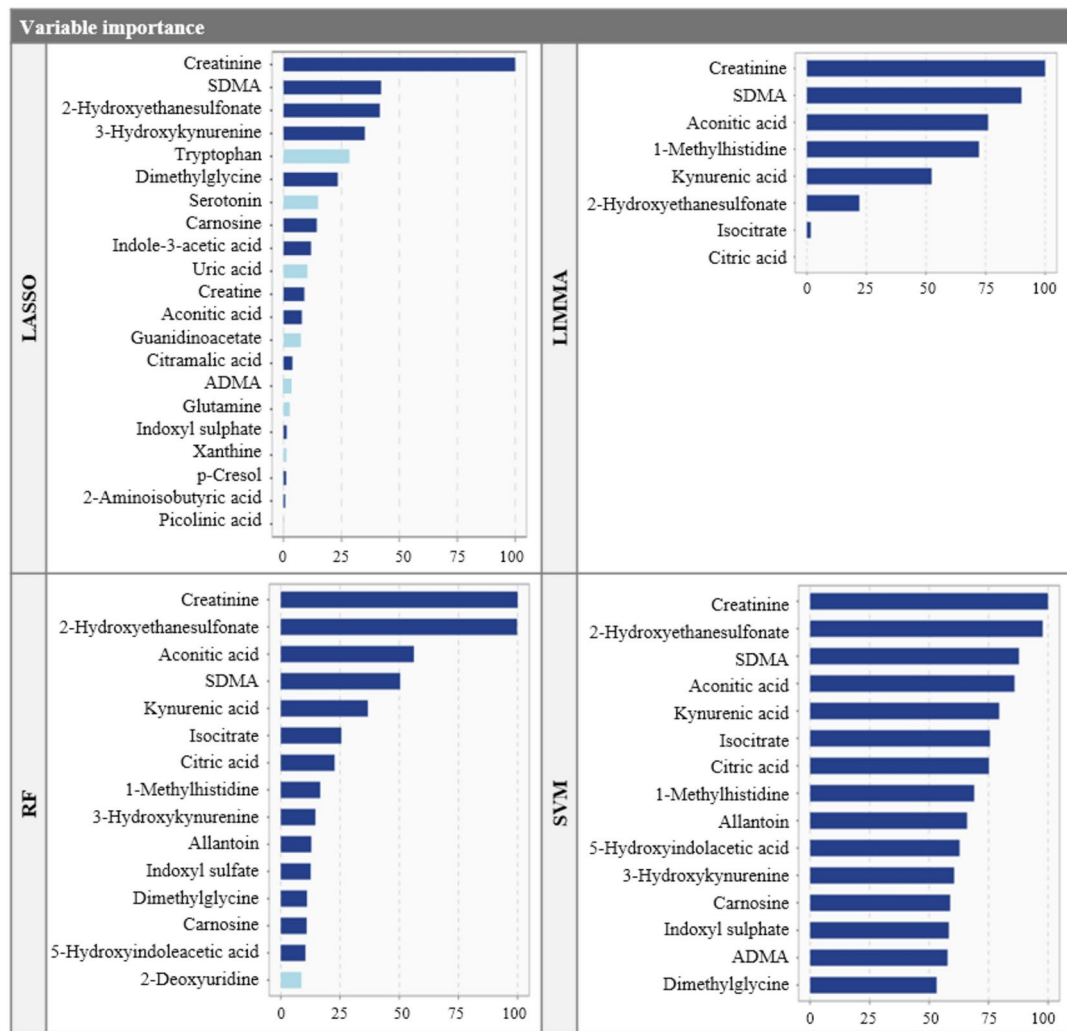


Fig. 3. Variable importance of the selected serum metabolites resulting from LASSO regression and LIMMA with subsequent GLM, and the top 15 metabolites from the RF and SVM models. The relative importance of each metabolite is quantified by assigning a weight between 0 and 100. Metabolites exhibiting higher values are deemed to exert greater influence within the model. Dark blue represents increased metabolites, while light blue indicates a decrease in the CKD2 population. ADMA asymmetric dimethylarginine.

metabolism³⁰. The human CKD metabolomics study of Boelaert et al. (2017) identified 2-hydroxyethanesulfonate as a novel uremic solute and reported its downregulation in urine, while our results suggest elevated levels in both serum and urine in feline CKD³¹. Despite the absence of a definitive explanation for these contradictory findings, we postulate that these may stem from fundamental differences in taurine metabolism between species. More specifically, cats exhibit a markedly reduced capacity to synthesize taurine, rendering it an essential amino acid³². While humans can utilize both taurine and glycine in the synthesis of conjugated bile acids, cats almost exclusively employ taurine³³. Moreover, as the feline urinary excretion mechanism of 2-hydroxyethanesulfonate has not been described yet in detail, we can only hypothesize that these discrepancies may be of influence. Additionally, Kimura et al. (2016) highlighted elevated plasma levels of 2-hydroxyethanesulfonate as a predictor for end-stage human CKD³⁴, in line with the increased serum concentrations from our study. Moreover, patients in the top tertile ($n=3$) of this metabolite had the highest adjusted hazard ratio compared to the other significant metabolite predictors.

The citric acid cycle (TCA) intermediate aconitic acid was identified in all multivariate and ML-based predictive models. Its *cis*-isomer is formed from citrate by the enzyme aconitase, which is then converted into isocitrate. Given the high sensitivity of aconitase to oxidative damage³⁵, its activity has been reported to be reduced in rats and mice with CKD as a result of the corresponding oxidative stress^{36,37}. In addition, aconitase activity has been shown to decline with a decreasing kidney function³⁸. *Trans*-aconitic acid is a non-enzymatic byproduct of *cis*-aconitic acid. By inhibiting the aconitase enzyme, it suppresses the TCA cycle and respiration in tissues and induces reactive oxygen species, causing oxidative stress and cell damage^{39,40}. A significant association of *cis*- and *trans*-aconitic acid with renal function has been reported in several human studies^{39,41,42}, suggesting their potential as a candidate biomarker for the detection of early CKD.

Model	Timepoint	AUC	CI	Accuracy	CI
LASSO (n=5)	T ₀	0.989	0.965–1.000	0.967	0.828–0.999
	T ₋₆	0.864	0.724–1.000	0.759	0.565–0.897
	T ₋₁₂	0.766	0.595–0.938	0.724	0.528–0.873
LIMMA (n=12)	T ₀	1.000	1.000–1.000	0.967	0.828–0.999
	T ₋₆	0.877	0.753–1.000	0.793	0.603–0.920
	T ₋₁₂	0.818	0.667–0.969	0.724	0.528–0.873
RF	T ₀	0.979	0.934–1.000	0.933	0.779–0.992
	T ₋₆	0.864	0.729–0.999	0.793	0.603–0.920
	T ₋₁₂	0.740	0.559–0.992	0.759	0.565–0.897
SVM linear	T ₀	0.984	0.949–1.000	0.967	0.828–0.999
	T ₋₆	0.929	0.826–1.000	0.862	0.683–0.961
	T ₋₁₂	0.792	0.621–0.963	0.759	0.565–0.897
SVM radial	T ₀	0.984	0.949–1.000	0.967	0.828–0.999
	T ₋₆	0.929	0.826–1.000	0.828	0.642–0.942
	T ₋₁₂	0.838	0.683–0.992	0.724	0.528–0.873

Table 6. Predictive performance of multivariate and ML-based models developed using serum metabolites and clinical parameters. AUC and accuracy were evaluated at T₋₁₂, T₋₆ and T₀.

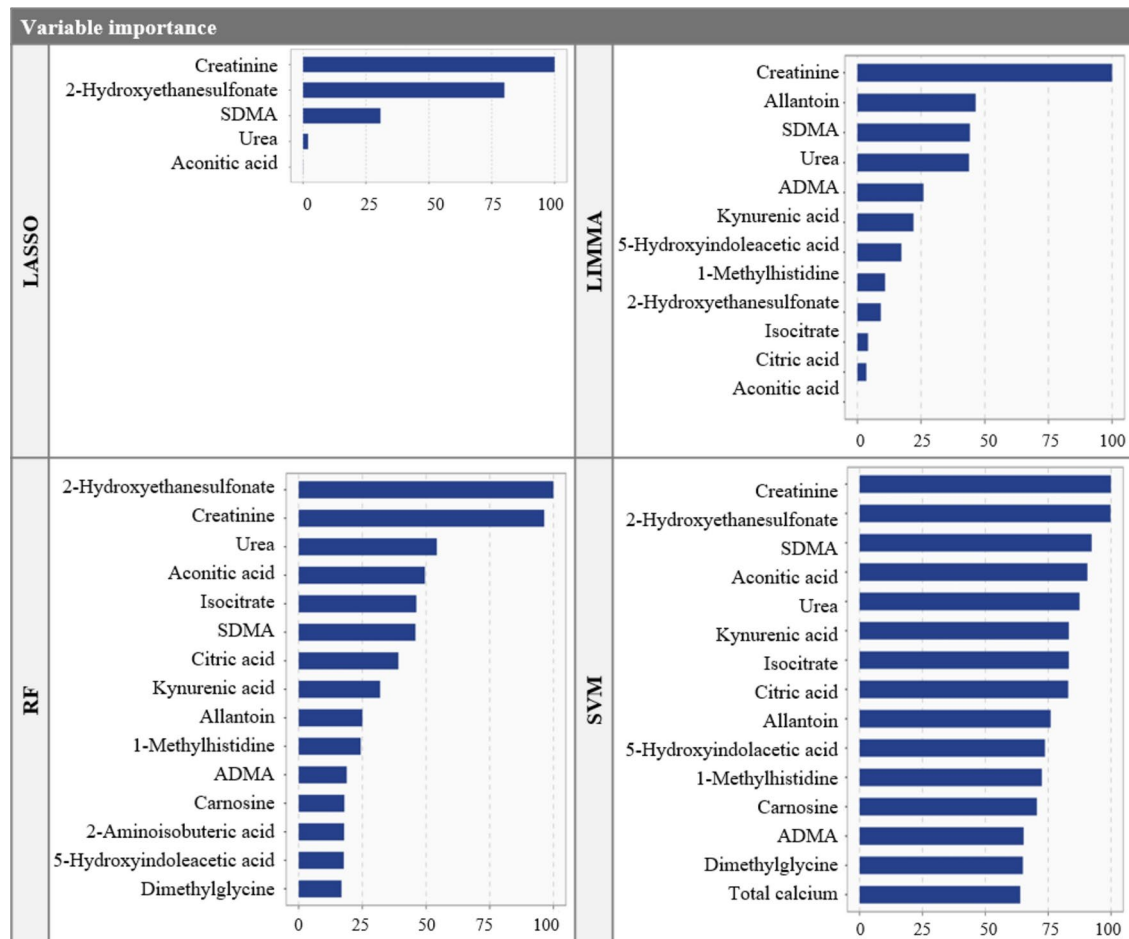


Fig. 4. Variable importance of the selected serum metabolites and clinical parameters resulting from LASSO regression and LIMMA with subsequent GLM, RF and SVM models. For the latter two, only the top 15 variables are presented. The relative importance of each variable is quantified by assigning a weight between 0 and 100. Variables exhibiting higher values are deemed to exert greater influence within the model. All presented variables were increased in the CKD2 population.

Finally, serum SDMA and creatinine also exerted high variable importance in all multivariate and ML-based models. Moreover, when incorporating the clinical parameters to the model building phase, urea was also identified as an important metabolite in CKD2 prediction. While SDMA has been proposed as an early stand-alone biomarker for CKD diagnosis, the study of Brans et al. (2021) already demonstrated that the sensitivity of plasma SDMA as an individual biomarker is not superior over creatinine in azotemic and non-azotemic cats.¹⁰ Our study also demonstrated that other promising metabolites, including 3-hydroxykynurenine, exhibited enhanced predictive capabilities in comparison to SDMA at T₋₆. Despite SDMA being the 4th best predictor based on AUC at T₋₁₂, it is important to keep in mind that the models were trained using the baseline population, in which the group classification was based on SDMA and creatinine values, leading to a perfect separation. However, similar as to Brans et al. (2021), our study also demonstrated poor sensitivity values for SDMA on T₀, T₋₆ and T₋₁₂ (0.571, 0.350 and 0.400, respectively), thereby corroborating their assertion regarding the limited added value of SDMA as a single diagnostic biomarker. Although creatinine is regarded as a rather late individual biomarker for CKD diagnosis^{5,12}, our results revealed accurate diagnosis in the non-azotemic stage when creatinine is combined with other metabolites in the multivariate and ML-based models, similar to SDMA. While Finch et al. (2018) proposed serum creatinine as a more useful marker for serial monitoring of renal function in azotemic cats, we did not assess the longitudinal changes of this or other metabolites, as our models were constructed using the cross-sectional data of the baseline population⁴³. Although models could also be developed using the longitudinal data, thereby taking into account longitudinal changes in metabolite concentrations, we elected to proceed in the opposite manner. This approach would enable us to obtain a more adequate sample size and to conduct longitudinal evaluation of predictive performance in an independent population. As for urea, while this metabolite can be influenced by extrarenal factors (i.e. protein-rich diet), gastrointestinal bleeding, increased protein metabolism through clinical conditions such as infections and fever, malnutrition, and certain medication (i.e., glucocorticoids and tetracyclines), it enhanced AUC and accuracy of the multivariate and ML-based model. Urea was also incorporated in the predictive model for feline CKD of Bradley et al. (2019), together with creatinine, USG and age in a recurrent neural network model, resulting in a high specificity (99%) but moderate sensitivity (63%) one year before diagnosis⁴⁴.

Notably, while pairwise comparisons revealed more significant metabolic alterations in urine and ratios of both matrices (i.e. S/U and U/S), especially on T₋₆, multivariate statistics and ML-based models demonstrated superior predictive performance when utilizing serum metabolites. This can be explained by the inherent strengths of multivariate and ML-based approaches. Although individual metabolites may not show significance alone, their combined effects can reveal patterns that distinguish CKD from healthy states.

One of the most recently published studies regarding metabolomics in early feline CKD is that of Nealon et al. (2024), identifying lipids and amino acids as the primary discriminant metabolite classes between healthy cats and cats with CKD1-2, using untargeted metabolomics¹⁵. Although lipids were not included in our targeted panel, there were some similarities regarding significantly altered (histidine, trimethylamine-N-oxide, tryptophan and valine) and non-significantly altered (choline, leucine, lysine, methionine) amino acids when performing univariate comparisons. However, while our study identified significantly different concentrations of indoxyl sulphate, isoleucine, p-cresol sulphate and taurine, this was not the case in the aforementioned study. In contrast, the study identified significant alterations in arginine and phenylalanine, which could not be confirmed in our study. Besides CKD2 (n=14), their population also included CKD1 cats (n=3), which could influence the mean concentration of certain metabolites, leading to discrepant results in univariate pairwise comparisons. Furthermore, sample sizes were limited and there was a paucity of feline-specific optimised and validated serum extraction and analysis protocols. As they propose further investigation of these metabolites as potential early biomarkers for feline CKD, our study makes a significant contribution to this field by not only evaluating single metabolites as potential biomarkers, but also assessing metabolite and matrix ratios, and metabolite panels in both serum and urine. Moreover, our study transcends the limitations of a cross-sectional study design by evaluating performance in an independent longitudinal population, preceding the point of traditional CKD diagnosis.

Despite the potential of metabolomic analysis to elucidate biochemical pathways and discover biomarkers, translating metabolomic findings into routine clinical assays faces obstacles. Mass spectrometry (MS) platforms, while powerful, are hindered by labour-intensive sample preparation and the duration of analytical runs^{45,46}. However, emerging ambient ionisation techniques enable direct analysis of crude samples, thereby simplifying diagnostics and expanding screening capabilities to detect e.g. early renal deterioration, in combination with other diseases⁴⁷. Moreover, liquid chromatography-mass spectrometry (LC-MS) platforms are already employed by commercial laboratories for a number of routine tests, including the measurement of SDMA (Medvet, Antwerp), as was done in this study. While these types of platforms are particularly interesting in the measurement of multiple metabolites, other analytical approaches such as enzyme-linked immunoassays may be applied for individual biomarkers, as already commercially available for human and mouse 3-hydroxykynurenine in serum, plasma and body fluids. In view of the availability of such assays, the measurement of the aforementioned metabolites could be integrated into regular longitudinal health screenings for senior cats, in accordance with the recommendations set forth by the Feline Senior Care Guidelines of the American Association of Feline Practitioners (AAFP)⁴⁸.

One of the key strengths of our study is the use of two independent cohorts: a baseline population for biomarker discovery and model training, and a longitudinal population for model testing and validation. The baseline population consisted of CKD2 cats, who were allowed to receive a renal diet or CKD medication. This inclusion introduced the potential for variability in the metabolome due to dietary and medication influences, which may be a contributing factor to the observed discrimination between the healthy and CKD2 group⁴⁹. However, as none of the study patients in the longitudinal population received any therapeutic interventions during the follow-up period, we hypothesized that although dietary and/or pharmacological interventions can

lead to metabolic variations⁵⁰, they are not suspected to be the primary drivers of the observed discrimination between the metabolomes, as accurate predictions could be made on the longitudinal population using the baseline model. Although the sample sizes were too limited to perform statistical comparisons for each type of therapeutic intervention, the successful validation of our proposed biomarkers in this cohort may suggest that they are robust and specific to renal pathology, irrespective of external dietary or pharmacological influences. However, additional studies are required to statistically elucidate the effect of therapeutic interventions.

It is also important to consider the relatively small sample size, although larger than that of previous metabolomics studies in feline CKD^{12,14,15,49,51,52}. Furthermore, whereas IRIS guidelines define CKD IRIS stage 1 (CKD1) as the earliest stage, only cats with CKD2 were included. Diagnosis of CKD1 is based on renal abnormalities such as poorly concentrated urine, persistent proteinuria, abnormal renal imaging results, or consistently elevated SDMA levels, in the absence of renal azotemia and clinical signs^{17,53}. However, these changes are not specific for feline CKD, making accurate diagnosis of CKD1 challenging, which may result into less reliable models when used for model development⁵. On the other hand, it is not excluded that CKD2 cats from the longitudinal might already have CKD1 at T₆, which could lead to overestimations of performance. Additionally, the absence of GFR measurements and renal ultrasonography further restricted the ability to detect these potential CKD1 cats. Finally, the selection of candidate biomarkers was based on previous knowledge from human and rodent studies^{31,54–59}. This metabolic profiling approach ensured accurate compound annotation but might not fully capture the unique metabolic signatures of feline CKD, limiting the panel's efficacy. Although metabolic fingerprinting could aid in this, compound annotation still remains the greatest bottleneck⁶⁰. Despite these challenges, our targeted analysis revealed several key metabolites that show potential in predicting feline CKD.

Despite the absence of evidence indicating that diagnosing CKD and thus initiating treatment at an earlier stage, prior to CKD1, can enhance clinical outcomes or prognosis, Lees et al. have postulated that prompt intervention may influence the progression rate and extend lifespan⁴. It is therefore important to ascertain whether therapeutic interventions at an even earlier stage of CKD may result in further improvements in clinical outcome.

Conclusions

This study highlights the potential of metabolomics in addressing the diagnostic challenges associated with early feline CKD. By employing a targeted metabolomic approach, we detected several metabolites and metabolite ratios that exhibit significant alterations in cats with CKD2. By incorporating univariate and multivariate statistical analyses and ML-based techniques, we developed predictive models that can accurately distinguish between healthy cats and those with CKD2. The results demonstrated that specific individual metabolites, particularly S/U 3-hydroxykynurenine, showed significant potential as early biomarkers of CKD, with an accuracy of 0.804 and AUC of 0.844, six months prior to traditional diagnosis. Linear support vector machine-based ML modelling employing metabolites and clinical parameters resulted in an even higher AUC of 0.929, and accuracy of 0.862. In addition, consistent identification of key serum metabolites based on variable importance was demonstrated, including creatinine, SDMA, urea, 2-hydroxyethanesulfonate, andaconitic acid. These findings pave the way for improved diagnostic tools, ultimately contributing to better disease management for affected cats. Future studies to determine the specificity and influence of comorbidities including hyperthyroidism are warranted to validate these findings and explore the practical implementation of metabolomic diagnostics in veterinary medicine.

Methods

Ethics declarations

The research protocol received approval from the ethical committees of the Faculties of Veterinary Medicine and Bioscience Engineering for animal ethics (EC2020-081), the Committee for Medical Ethics for human ethics (EC2024-26), and the deontological committee. For animal ethics, all procedures were approved by the above mentioned institution and performed in accordance with the relevant guidelines and regulations, including the ARRIVE guidelines (Animal Research: Reporting of In Vivo Experiments). In addition, procedures were approved by the above-mentioned institution for human ethics and conducted in accordance with the relevant guidelines and regulations. Owners were informed about the objectives of the study and provided informed consent.

Study population and design

Cats included in this study were privately-owned and proactively recruited via the Small Animal Clinic at the Faculty of Veterinary Medicine, Ghent University, and through first- and second-line veterinary practices (n=15), located in Flanders, Belgium. For the latter, a mobile team from the Small Animal Clinic visited the practices on-site to perform health screenings including sample collection. Control visits were performed every six months for two years, according to the 2021 feline life stage guidelines for senior cats⁶¹. All samples were retrospectively selected from the follow-up cohort, containing healthy cats and cats with previously diagnosed CKD at enrolment. The latter ones were selected as CKD2 cats for the baseline population, since no samples were available from a previous healthy state. For the CKD2 cats in the longitudinal population, cats were included that had control visits six and twelve months before first CKD diagnosis. There were no common cats in both study populations. Physical examination including blood pressure measure, complete blood count, serum biochemistry including total thyroxine (T4), infectious serological testing (feline leukaemia virus and feline immunodeficiency virus, only tested on first visit) and urinalysis (including dip stick testing, UPC, USG, microscopic sediment analysis, and bacterial culture) were performed in all cats to assess general health status^{62–66}. Owners were asked to complete a questionnaire related to their cat's health status, living environment,

daily activity, feeding practices, and disease history (Supplementary information). Cats receiving medication (except CKD-related medication for the CKD cats, i.e. angiotensin-converting enzyme inhibitors, angiotensin receptor blockers, phosphate binders and amlodipine) within one month prior to inclusion were excluded. CKD diagnosis was based on a compatible history and physical examination combined with appropriate laboratory findings (i.e. renal azotemia $> 161.8 \mu\text{mol/L}$ as defined by Ghys et al.⁶⁷ and USG $< 1.035^5$). Subsequently, only cats with CKD IRIS stage 2 were selected. To be included as a healthy cat, the above examinations could not reveal any clinically relevant abnormalities, except for a non-persistent decrease of USG (< 1.035) or increased UPC (> 0.4) of non-renal origin. Cats were excluded from the healthy group if, after a 6-month follow-up, they showed an increase in creatinine or SDMA within (i.e. exceeding their biologic variation⁶⁸) or above the reference interval, if they maintained suboptimal USG values, or if they developed proteinuria that could not be attributed to a post-renal cause (i.e. lower urinary tract inflammation or hemorrhage during cystocentesis). For CKD cats, CKD-related abnormalities were allowed (e.g., hypertension, hyperphosphatemia and proteinuria), but no significant comorbidities (e.g., hyperthyroidism, IBD, neoplasia).

Sample collection

Both urine and serum samples were obtained within a time frame of 15 min. Sterile urine was obtained through ultrasound-guided cystocentesis using a 10 mL syringe with a 22-gauge needle. Serum samples were collected via jugular or cephalic venipuncture using a 5 mL syringe with a 23-gauge needle. Subsequently, the urine and serum samples underwent centrifugation ($447 \times g$ for 3 min at room temperature, $2190 \times g$ for 5 min at 2°C , respectively). The resulting supernatants were aliquoted into plastic Eppendorf® tubes and stored at -80°C until further analysis.

Reagents and chemicals

Deuterium-labelled internal standards (Supplementary Table S8) and analytical reference standards (Supplementary Table S9) were obtained from Sigma-Aldrich (St-Louis, Missouri, USA), LGC standards (Teddington, London, UK) and MedChemExpress MCE (New Jersey, Princeton, USA). Solvents including acetone, acetonitrile (ACN) and methanol (MeOH) were purchased from Fisher Scientific (Loughborough, UK) and VWR International (Darmstadt, Germany). Ultrapure water (UPW) was obtained via the Arium® 611UV purification system from Sartorius (Göttingen, Germany).

Instrumentation

The instrumental method involved the utilization of ultra high-performance liquid chromatography coupled with quadrupole orbitrap high-resolution mass spectrometry (UHPLC-Q-Orbitrap HRMS), in accordance with the metabolomics protocol outlined in the publication by Vanden Broecke et al.⁶⁹. Chromatographic separation was performed using a Dionex UltiMate 3000 XRS UHPLC system (Thermo Fisher Scientific, San José, CA, USA), equipped with an Acquity HSS C18 column T3 (1.8 μm , 150 mm \times 2.1 mm) (Waters, Manchester, UK). A consistent column oven temperature of 45°C was maintained. A binary solvent system was employed, utilizing a gradient elution program at a constant flow rate of 0.4 ml/min consisting of UPW and ACN, both acidified with 0.1% formic acid. Samples were injected at a volume of 10 μL , with a maximum injection time of 150 μs . For the HRMS, a Thermo Fisher Scientific Exploris 120 Q-Orbitrap benchtop mass spectrometer (San José, CA, USA) was employed. The analysis was preceded by heated electrospray ionization (HESI-II source) in polarity switching mode. The mass scan range spanned from 50 to 800 Da, with a mass resolution of 120,000 full width at half maximum at 1 Hz.

For each matrix, sample extracts were pooled and included as Quality Control (QC) samples in duplicate after every ten samples throughout the analytical run. At the beginning, middle and end of the analysis, a mixture of analytical standards (Supplementary Table S9) was injected to verify the operational performance of the instrument and gather data for metabolite annotation. A panel of endogenous metabolites was selected based on their biological relevance in CKD, as described in previous reports on important urinary and serum metabolites in humans and rodents with CKD^{31,54–59}.

Analytical method

The extraction and analysis methods for serum and urine samples (Supplementary information) consisted of matrix- and species-specific in-house protocols. Targeted ($n=77$ metabolites) and untargeted ($n=1,949$ features) validation of the serum method showed excellent precision (i.e., instrumental, intra-assay and inter-day) (coefficient of variation (CV) $\leq 15\%$ or 30%, respectively), satisfactory linearity (coefficient of determination (R^2) ≥ 0.99 or 0.90, respectively) and an appropriate targeted recovery, ranging between 70 and 130%. For the targeted ($n=70$ metabolites) and untargeted ($n=2,348$ features) validation of the urinary protocol, exquisite instrumental and intra-assay precision were noted (CV $\leq 15\%$ or 30%, respectively)⁶⁹.

Data processing

Targeted data processing was performed by Xcalibur™ 3.0 (Thermo Fisher Scientific, San José, CA, USA). Annotation was performed comparing the mass-to-charge ratio (m/z -value), retention time (Rt) and $^{13}\text{C}/^{12}\text{C}$ isotope ratio with analytical standards, applying a mass deviation ≤ 5 ppm, maximum retention time shift of 2.5% and signal-to-noise ratio $\leq 10^{70–72}$. Additionally, to confirm targeted metabolite annotation, MS/MS fragmentation was performed on urinary and serum QC samples ($n=5$ for both matrices) and authentic reference standards using three different collision energies (i.e., 30, 50, and 70 eV). To ensure the quality and reliability of the serum and urinary metabolomics data, normalization was performed using the average signal of two consecutive QC samples to correct for instrumental drift. In multivariate statistical analysis and ML-based modelling, logarithmic transformation and Pareto scaling ($1/\sqrt{\text{SD}}$, where SD represents the standard deviation)

were applied to induce normality and standardize the range of peak intensities⁷³. As SDMA was not included in the targeted metabolomics panel, LC–MS abundances were utilized from the commercial laboratory (Medvet, Antwerp) that was initially engaged to perform the health screenings.

Data analysis

Statistical and ML-based data analysis were performed using R (version 2023.03.0)⁷⁴. In order to comprehensively map metabolic alterations associated with CKD, univariate statistical analysis was undertaken as an initial exploratory step in both matrices. This approach sought to identify individual metabolites that exhibit significant statistical differences between healthy and CKD affected cats. For the pairwise comparisons, either a Welch two-sample t test (parametric data) or Wilcoxon rank-sum test (non-parametric data) was employed. FDR corrected P-values (<0.05) for multiple testing were calculated following the Benjamini–Hochberg procedure⁷⁵. In addition to individual metabolites, ratios of metabolites within CKD-associated pathways were computed, encompassing the tryptophan metabolism (including the indole, kynurenine and serotonin pathway), the urea cycle, the carnitine and purine metabolism. Furthermore, ratios of the same metabolite in both matrices were computed. This dynamic approach has the potential to provide insights into the intricate processes of renal filtration and tubular function⁷⁶. Univariate statistical analysis was employed for all metabolites including metabolite and matrix ratios, while the ratios were omitted from multivariate and ML-based analysis to circumvent confounding effects through correlation. Unsupervised principal component analysis (PCA-X) was utilized to assess natural clustering among analysed samples, identify outliers, and confirm instrument stability using QC samples.

To develop a model, the first step was to compare metabolite abundances from the baseline population (healthy n = 61, CKD2 n = 63), retain the predictive features and determine the metabolite coefficients. Consequently, this model was evaluated in an independent longitudinal population (healthy n = 26, CKD2 n = 22). This allowed us to assess the predictivity of the model in a new population to and avoid overestimation of performance and as such ensure that our findings were eligible for generalization. Additionally, this longitudinal evaluation enabled the determination of the predictive capacity of the models across multiple timepoints (i.e., T₋₁₂, T₋₆ and T₀).

For the development of predictive panel with a subset of metabolites, two feature selection methods with subsequent modelling were compared. In order to create a predictive model with a subset of the a priori selected endogenous metabolites and ratios, both LASSO regression and LIMMA with subsequent GLM modelling were applied. LASSO has been demonstrated to be effective in both predictive modelling and the selection of metabolites^{77,78}. By introducing a penalty term lambda (λ) during model estimation, LASSO pushes regression coefficients of correlated or unimportant independent variables to zero, thereby falling out of the model⁷⁹. LIMMA is a software package developed within the R/Bioconductor framework. Although originally designed to facilitate differential expression analysis in the context of RNA-sequencing and microarray studies, it is now being employed in a growing number of other applications, including metabolomics, due to similar data types (i.e., small sample sizes with a large number of features)^{80,81}. The *topTable* function from the *limma* package was employed to construct models comprising the top-ranked metabolites (n = 2–10) according to their FDR corrected P-value.

Predictive models were also built with ML techniques, including RF and SVM, using the entire dataset. For SVM, both the simple linear kernel (further referred to as ‘SVM linear’) for straight-line data and radial basis function kernel (further referred to as ‘SVM radial’) for more complex patterns were employed⁸². These ML algorithms have been among the most frequently employed algorithms in metabolomic studies⁸³, including for the successful development of predictive models for human CKD^{84–86}.

In addition to the metabolites from the targeted metabolomics panel, the clinical parameters from Table 1 (i.e., age, SBP, BCS, MCS, UPC, USG, urinary culture, urea, albumin, phosphate, total calcium and potassium) were also incorporated into the model building phase in a subsequent data analysis experiment, to ascertain whether these variables could enhance its predictive capacity.

The R *caret* package was employed for all univariate, multivariate and ML-based modelling. The optimal hyperparameters were identified through a tenfold cross-validation procedure based on the model’s predictive accuracy⁸⁷. This was also performed for λ to determine shrinkage in LASSO regression, mtry for the number of variables at each split in RF and C for controlling the trade-off between maximizing the margin and minimizing training errors in SVM. Cross-validation was implemented using the *trainControl* function. In order to enable the corresponding statistical approach, the *method* argument of the *train* function was set as *glmnet* for LASSO regression, *glm* for GLM modelling following LIMMA, *rf* for RF, and *svmLinear* and *svmRadial* for SVM.

Data availability

The datasets generated and/or analysed during the current study are available from the corresponding author on reasonable request, as well as the R codes used for the statistical analysis.

Received: 4 October 2024; Accepted: 10 February 2025

Published online: 26 February 2025

References

1. Brown, C. A., Elliott, J., Schmiedt, C. W. & Brown, S. A. Chronic kidney disease in aged cats: clinical features, morphology, and proposed pathogeneses. *Vet. Pathol.* **53**, 309–326. <https://doi.org/10.1177/0300985815622975> (2016).
2. O’Neill, D. G., Church, D. B., McGreevy, P. D., Thomson, P. C. & Brodbelt, D. C. Longevity and mortality of cats attending primary care veterinary practices in England. *J. Feline Med. Surg.* **17**, 125–133. <https://doi.org/10.1177/1098612X14536176> (2015).
3. Paepe, D. *Screening for early feline chronic kidney disease: Limitations of currently available tests and possible solutions*. Doctor of Philosophy (PhD) thesis, Faculty of Veterinary Medicine, Ghent University (2014).

4. Lees, G. E. Early diagnosis of renal disease and renal failure. *Vet. Clin. N. Am. Small Anim. Pract.* **34**, 867–885. <https://doi.org/10.1016/j.cvsm.2004.03.004> (2004).
5. Paepe, D. & Daminet, S. Feline CKD: diagnosis, staging and screening - what is recommended?. *J. Feline Med. Surg.* **15**(Suppl 1), 15–27. <https://doi.org/10.1177/1098612x13495235> (2013).
6. Finch, N. Measurement of glomerular filtration rate in cats: methods and advantages over routine markers of renal function. *J. Feline Med. Surg.* **16**, 736–748. <https://doi.org/10.1177/1098612x14545274> (2014).
7. Quimby, J. M. Searching for biomarkers in feline chronic kidney disease: A new frontier. *Vet. J.* **206**, 3–4. <https://doi.org/10.1016/j.tjvjl.2015.05.005> (2015).
8. Sparkes, A. H. et al. ISFM consensus guidelines on the diagnosis and management of feline chronic kidney disease. *J. Feline Med. Surg.* **18**, 219–239. <https://doi.org/10.1177/1098612x16631234> (2016).
9. Hokamp, J. A. & Nabity, M. B. Renal biomarkers in domestic species. *Vet. Clin. Pathol.* **45**, 28–56. <https://doi.org/10.1111/vcp.12333> (2016).
10. Brans, M. et al. Plasma symmetric dimethylarginine and creatinine concentrations and glomerular filtration rate in cats with normal and decreased renal function. *J. Vet. Intern. Med.* **35**, 303–311. <https://doi.org/10.1111/jvim.15975> (2021).
11. Cowgill, L. D. et al. Is progressive chronic kidney disease a slow acute kidney injury?. *Vet. Clin. N. Am. Small Anim. Pract.* **46**, 995–1013. <https://doi.org/10.1016/j.cvsm.2016.06.001> (2016).
12. Hall, J., Yerramilli, M., Obare, E. & Jewell, D. Comparison of serum concentrations of symmetric dimethylarginine and creatinine as kidney function biomarkers in cats with chronic kidney disease. *J. Vet. Intern. Med.* **28**, 1676–1683. <https://doi.org/10.1111/jvim.12445> (2014).
13. Kongtasai, T. et al. Renal biomarkers in cats: A review of the current status in chronic kidney disease. *J. Vet. Intern. Med.* **36**, 379–396. <https://doi.org/10.1111/jvim.16377> (2022).
14. Rivera-Velez, S. & Villarino, N. Feline urine metabolomic signature: characterization of low-molecular-weight substances in urine from domestic cats. *J. Feline Med. Surg.* **20**, 155–163. <https://doi.org/10.1177/1098612x17701010> (2018).
15. Nealon, N. J., Summers, S., Quimby, J. & Winston, J. A. Untargeted metabolomic profiling of serum from client-owned cats with early and late-stage chronic kidney disease. *Sci. Rep.* **14**, 4755. <https://doi.org/10.1038/s41598-024-55249-5> (2024).
16. Elliott, J. & Watson, A. *Current Veterinary Therapy XV* 857–863 (Saunders-Elsevier, 2014).
17. IRIS. *IRIS staging of CKD*. www.iris-kidney.com/guidelines/staging.html (2023).
18. Zakrocka, I. & Zaluska, W. Kynurenone pathway in kidney diseases. *Pharmacol. Rep.* **74**, 27–39. <https://doi.org/10.1007/s43440-02-1-00329-w> (2021).
19. Mor, A., Kalaska, B. & Pawlak, D. Kynurenone pathway in chronic kidney disease: What's old, what's new, and what's next?. *Int. J. Tryptophan Res.* <https://doi.org/10.1177/1178646920954882> (2020).
20. Okuno, E. & Kido, R. Kynureinase and kynurenone 3-hydroxylase in mammalian tissues. *Adv. Exp. Med. Biol.* **294**, 167–176. https://doi.org/10.1007/978-1-4684-5952-4_15 (1991).
21. Badawy, A.A.-B. Kynurenone pathway of tryptophan metabolism: Regulatory and functional aspects. *Int. J. Tryptophan Res.* <https://doi.org/10.1177/1178646917691938> (2017).
22. Pawlak, K., Domaniewski, T., Mysliwiec, M. & Pawlak, D. The kynurenines are associated with oxidative stress, inflammation and the prevalence of cardiovascular disease in patients with end-stage renal disease. *Atherosclerosis* **204**, 309–314 (2009).
23. Pawlak, D., Tankiewicz, A. & Buczko, W. Kynurenone and its metabolites in the rat with experimental renal insufficiency. *J. Physiol. Pharmacol.* **52**, 755–766 (2004).
24. Tankiewicz, A., Pawlak, D., Topczewska-Bruna, J. & Buczko, W. Kidney and liver kynurenone pathway enzymes in chronic renal failure. *Adv. Exp. Med. Biol.* **527**, 409–414. https://doi.org/10.1007/978-1-4615-0135-0_48 (2003).
25. Pawlak, D., Tankiewicz, A., Matys, T. & Buczko, W. Peripheral distribution of kynurenone metabolites and activity of kynurenone pathway enzymes in renal failure. *J. Physiol. Pharmacol.* **54**, 175–189 (2024).
26. González Esquivel, D. et al. Kynurenone pathway metabolites and enzymes involved in redox reactions. *Neuropharmacology* **112**, 331–345. <https://doi.org/10.1016/j.neuropharm.2016.03.013> (2017).
27. Badawy, A.A.-B. Kynurenone pathway and human systems. *Exp. Gerontol.* <https://doi.org/10.1016/j.exger.2019.110770> (2020).
28. Wang, Q., Liu, D., Song, P. & Zou, M. H. Tryptophan-kynurenone pathway is dysregulated in inflammation, and immune activation. *Front. Biosci.* **20**, 1116–1143. <https://doi.org/10.2741/4363> (2015).
29. Fallarino, F. et al. T cell apoptosis by tryptophan catabolism. *Cell Death Differ.* **9**, 1069–1077. <https://doi.org/10.1038/sj.cdd.4401073> (2002).
30. Fellman, J. H., Roth, E. S., Avedovech, N. A. & McCarthy, K. D. The metabolism of taurine to isethionate. *Arch. Biochem. Biophys.* **204**, 560–567. [https://doi.org/10.1016/0003-9861\(80\)90068-5](https://doi.org/10.1016/0003-9861(80)90068-5) (1980).
31. Boelaert, J. et al. Metabolic profiling of human plasma and urine in chronic kidney disease by hydrophilic interaction liquid chromatography coupled with time-of-flight mass spectrometry: a pilot study. *Anal. Bioanal. Chem.* **409**, 2201–2211. <https://doi.org/10.1007/s00216-016-0165-x> (2017).
32. Che, D., Nyingwa, P. S., Ralinala, K. M., Maswanganye, G. M. T. & Wu, G. Amino acids in the nutrition, metabolism, and health of domestic cats. *Adv. Exp. Med. Biol.* **1285**, 217–231. https://doi.org/10.1007/978-3-03-54462-1_11 (2021).
33. Rabin, B., Nicolosi, R. J. & Hayes, K. C. Dietary influence on bile acid conjugation in the cat. *J. Nutr.* **106**, 1241–1246. <https://doi.org/10.1093/jn/106.9.1241> (1976).
34. Kimura, T. et al. Identification of biomarkers for development of end-stage kidney disease in chronic kidney disease by metabolomic profiling. *Sci. Rep.* **6**, 1–8. <https://doi.org/10.1038/srep26138> (2016).
35. Lushchak, O. V., Piroddi, M., Galli, F. & Lushchak, V. I. Aconitase post-translational modification as a key in linkage between Krebs cycle, iron homeostasis, redox signaling, and metabolism of reactive oxygen species. *Redox Rep.* **19**, 8–15. <https://doi.org/10.1179/1351000213Y.0000000073> (2014).
36. Mapuskar, K. A. et al. Persistent increase in mitochondrial superoxide mediates cisplatin-induced chronic kidney disease. *Redox Biol.* **20**, 98–106. <https://doi.org/10.1016/j.redox.2018.09.020> (2019).
37. Correa, F. et al. Curcumin maintains cardiac and mitochondrial function in chronic kidney disease. *Free Radic. Biol. Med.* **61**, 119–129. <https://doi.org/10.1016/j.freeradbiomed.2013.03.017> (2013).
38. Yarian, C. S., Torosov, D. & Sohal, R. S. Aconitase is the main functional target of aging in the citric acid cycle of kidney mitochondria from mice. *Mech. Ageing Dev.* **127**, 79–84. <https://doi.org/10.1016/j.mad.2005.09.028> (2006).
39. Toyohara, T. et al. Metabolomic profiling of uremic solutes in CKD patients. *Hypertens. Res.* **33**, 944–952. <https://doi.org/10.1038/hrr.2010.113> (2010).
40. Villafranca, J. J. The mechanism of aconitase action. Evidence for an enzyme isomerization by studies of inhibition by tricarboxylic acids. *J. Biol. Chem.* **249**, 6149–6155 (1974).
41. Rhee, E. et al. A combined epidemiologic and metabolomic approach improves CKD prediction. *J. Am. Soc. Nephrol.* **24**, 1330–1338 (2013).
42. Suzuki, T. et al. Transcriptional regulation of organic anion transporting polypeptide SLCO4C1 as a new therapeutic modality to prevent chronic kidney disease. *J. Pharm. Sci.* **100**, 3696–3707. <https://doi.org/10.1002/jps.22641> (2011).
43. Finch, N. C., Syme, H. M. & Elliott, J. Repeated measurements of renal function in evaluating its decline in cats. *J. Feline Med. Surg.* **20**, 1144–1148. <https://doi.org/10.1177/1098612X18757591> (2018).
44. Bradley, R. et al. Predicting early risk of chronic kidney disease in cats using routine clinical laboratory tests and machine learning. *J. Vet. Intern. Med.* **33**, 2644–2656. <https://doi.org/10.1111/jvim.15623> (2019).

45. Kole, P. L., Venkatesh, G., Kotecha, J. & Sheshala, R. Recent advances in sample preparation techniques for effective bioanalytical methods. *Biomed. Chromatogr.* **25**, 199–217. <https://doi.org/10.1002/bmc.1560> (2011).
46. Vuckovic, D. Current trends and challenges in sample preparation for global metabolomics using liquid chromatography–mass spectrometry. *Anal. Bioanal. Chem.* **403**, 1523–1548. <https://doi.org/10.1007/s00216-012-6039-y> (2012).
47. Plekhova, V., De Windt, K., De Spiegeleer, M., De Graeve, M. & Vanhaecke, L. Recent advances in high-throughput biofluid metabotyping by direct infusion and ambient ionization mass spectrometry. *TrAC* **168**, 117287 (2023).
48. Ray, M. et al. 2021 AAFP feline senior care guidelines. *J. Feline Med. Surg.* **23**, 613–638. <https://doi.org/10.1177/1098612X211021538> (2021).
49. Ruberti, B. et al. Serum metabolites characterization produced by cats CKD affected, at the 1 and 2 stages, before and after renal diet. *Metabolites* **13**, 43. <https://doi.org/10.3390/metabolite13010043> (2022).
50. Mertowska, P. et al. A link between chronic kidney disease and gut microbiota in immunological and nutritional aspects. *Nutrients* **13**, 3637. <https://doi.org/10.3390/nut13103637> (2021).
51. Finch, N. et al. Preliminary demonstration of benchtop NMR metabolic profiling of feline urine: chronic kidney disease as a case study. *BMC Res. Notes* **14**, 1–5. <https://doi.org/10.1186/s13104-021-05888-y> (2021).
52. Hall, J. A., Jackson, M. I., Jewell, D. E. & Ephraim, E. Chronic kidney disease in cats alters response of the plasma metabolome and fecal microbiome to dietary fiber. *PLoS One* <https://doi.org/10.1371/journal.pone.0235480> (2020).
53. Sargent, H. J., Elliott, J. & Jepson, R. E. The new age of renal biomarkers: does SDMA solve all of our problems?. *J. Small Anim. Pract.* <https://doi.org/10.1111/jsap.13236> (2021).
54. Zhang, G., Saito, R. & Sharma, K. A metabolite-GWAS (mGWAS) approach to unveil chronic kidney disease progression. *Kidney Int.* **91**, 1274–1276. <https://doi.org/10.1016/j.kint.2017.03.022> (2017).
55. Hayashi, K. et al. Use of serum and urine metabolome analysis for the detection of metabolic changes in patients with stage 1–2 chronic kidney disease. *Nephrorol. Mon.* **3**, 164–171 (2023).
56. Kalantari, S. & Nafar, M. An update of urine and blood metabolomics in chronic kidney disease. *Biomark. Med.* **13**, 577–597. <https://doi.org/10.2217/bmm-2019-0008> (2019).
57. Zhao, Y. Y., Liu, J., Cheng, X. L., Bai, X. & Lin, R. C. Urinary metabolomics study on biochemical changes in an experimental model of chronic renal failure by adenine based on UPLC Q-TOF/MS. *Clin. Chim. Acta* **413**, 642–649. <https://doi.org/10.1016/j.cca.2011.12.012> (2012).
58. Govender, M. A., Brandenburg, J. T., Fabian, J. & Ramsay, M. The use of ‘omics for diagnosing and predicting progression of chronic kidney disease: A scoping review. *Front. Genet.* <https://doi.org/10.3389/fgene.2021.682929> (2021).
59. Rysz, J., Gluba-Brzózka, A., Franczyk, B., Jabłonowski, Z. & Ciałkowska-Rysz, A. Novel biomarkers in the diagnosis of chronic kidney disease and the prediction of its outcome. *Int. J. Mol. Sci.* <https://doi.org/10.3390/ijms18081702> (2017).
60. Gertsman, I. & Barshop, B. A. Promises and pitfalls of untargeted metabolomics. *J. Inherit. Metab. Dis.* **41**, 355–366. <https://doi.org/10.1007/s10545-017-0130-7> (2018).
61. Quimby, J. et al. 2021 AAHA/AAP feline life stage guidelines. *J. Feline Med. Surg.* **23**, 211–233. <https://doi.org/10.1177/1098612X21993657> (2021).
62. Acierno, M. J. et al. ACVIM consensus statement: Guidelines for the identification, evaluation, and management of systemic hypertension in dogs and cats. *J. Vet. Intern. Med.* **32**, 1803–1822. <https://doi.org/10.1111/jvim.15331> (2018).
63. Little, S. et al. 2020 AAFP Feline retrovirus testing and management guidelines. *J. Feline Med. Surg.* **22**, 5–30. <https://doi.org/10.1177/1098612X19895940> (2020).
64. Paepe, D. et al. Routine health screening: findings in apparently healthy middle-aged and old cats. *J. Feline Med. Surg.* **15**, 8–19. <https://doi.org/10.1177/1098612X12464628> (2013).
65. Reppas, G. & Foster, S. F. Practical urinalysis in the cat: 1: Urine macroscopic examination “tips and traps”. *J. Feline Med. Surg.* **18**, 190–202. <https://doi.org/10.1177/1098612X16631228> (2016).
66. Reppas, G. & Foster, S. F. Practical urinalysis in the cat: 2: Urine microscopic examination “tips and traps”. *J. Feline Med. Surg.* **18**, 373–385. <https://doi.org/10.1177/1098612X16643249> (2016).
67. Ghys, L. F. et al. Biological validation of feline serum cystatin C: The effect of breed, age and sex and establishment of a reference interval. *Vet. J.* **204**, 168–173. <https://doi.org/10.1016/j.tvjl.2015.02.018> (2015).
68. Prieto, J. M. et al. Biologic variation of symmetric dimethylarginine and creatinine in clinically healthy cats. *Vet. Clin. Pathol.* **49**, 401–406. <https://doi.org/10.1111/vcp.12840> (2020).
69. Vanden Broecke, E., Van Mulders, L., De Paepe, E., Daminet, S. & Vanhaecke, L. Optimization and validation of metabolomics methods for feline urine and serum towards application in veterinary medicine. *Anal. Chim. Acta* <https://doi.org/10.1016/j.aca.2024.342694> (2024).
70. Wijnant, K. et al. Validated ultra-high-performance liquid chromatography hybrid high-resolution mass spectrometry and laser-assisted rapid evaporative ionization mass spectrometry for salivary metabolomics. *Anal. Chem.* **92**, 5116–5124. <https://doi.org/10.1021/acs.analchem.9b05598> (2020).
71. FDA. Bioanalytical Method Validation Guidance for Industry. <https://www.fda.gov/regulatory-information/search-fda-guidance-documents/bioanalytical-method-validation-guidance-industry> (2018).
72. Rombouts, C., De Spiegeleer, M., Van Meulebroek, L., De Vos, W. H. & Vanhaecke, L. Validated comprehensive metabolomics and lipidomics analysis of colon tissue and cell lines. *Anal. Chim. Acta* **1066**, 79–92. <https://doi.org/10.1016/j.aca.2019.03.020> (2019).
73. van den Berg, R. A., Hoefsloot, H. C., Westerhuis, J. A., Smilde, A. K. & van der Werf, M. J. Centering, scaling, and transformations: Improving the biological information content of metabolomics data. *BMC Genom.* **7**, 142–157. <https://doi.org/10.1186/1471-2164-7-142> (2006).
74. R: A language and environment for statistical computing. <https://www.R-project.org/> (R Core Team, 2023).
75. Benjamini, Y. & Hochberg, Y. Controlling the false discovery rate: a practical and powerful approach to multiple testing. *J. R. Stat. Soc. Ser. B Stat. Methodol.* **57**, 289–300 (1995).
76. Soliman, S. A. et al. Exploring urine:serum fractional excretion ratios as potential biomarkers for lupus nephritis. *Front. Immunol.* <https://doi.org/10.3389/fimmu.2022.910993> (2022).
77. Ng, D. P. et al. A metabolomic study of low estimated GFR in non-proteinuric type 2 diabetes mellitus. *Diabetologia* **55**, 499–508. <https://doi.org/10.1007/s00125-011-2339-6> (2012).
78. Chan, A. W. et al. (1)H-NMR urinary metabolomic profiling for diagnosis of gastric cancer. *Br. J. Cancer* **114**, 59–62. <https://doi.org/10.1038/bjc.2015.414> (2016).
79. Xi, L. J., Guo, Z. Y., Yang, X. K. & Ping, Z. G. Application of LASSO and its extended method in variable selection of regression analysis. *Chin. J. Prev. Vet. Med* **57**, 107–111. <https://doi.org/10.3760/cma.j.cn112150-20220117-00063> (2023).
80. Ritchie, M. E. et al. limma powers differential expression analyses for RNA-sequencing and microarray studies. *Nucleic Acids Res.* **43**, e47. <https://doi.org/10.1093/nar/gkv007> (2015).
81. Castellano-Escuder, P., González-Domínguez, R., Carmona-Pontaque, F., Andrés-Lacueva, C. & Sánchez-Pla, A. POMA shiny: A user-friendly web-based workflow for metabolomics and proteomics data analysis. *PLoS Comput. Biol.* **17**, e1009148. <https://doi.org/10.1371/journal.pcbi.1009148> (2021).
82. Ben-Hur, A., Ong, C. S., Sonnenburg, S., Schölkopf, B. & Rätsch, G. Support vector machines and kernels for computational biology. *PLoS Comput. Biol.* **4**, e1000173. <https://doi.org/10.1371/journal.pcbi.1000173> (2008).
83. Galal, A., Talal, M. & Moustafa, A. Applications of machine learning in metabolomics: Disease modeling and classification. *Front. Genet.* <https://doi.org/10.3389/fgene.2022.1017340> (2022).

84. Debal, D. A. & Sitote, T. M. Chronic kidney disease prediction using machine learning techniques. *J. Big Data* **9**, 1–19. <https://doi.org/10.1186/s40537-022-00657-5> (2022).
85. James, N. & Kaushik, J. In *2nd International Conference on Advance Computing and Innovative Technologies in Engineering (ICACITE)*, 1134–1139 (Greater Noida, India, 2022).
86. Shanthakumari, A. S. & Jayakarthik, R. Utilizing support vector machines for predictive analytics in chronic kidney diseases. *Mater. Today Proc.* **81**, 951–956. <https://doi.org/10.1016/j.matpr.2021.04.309> (2023).
87. Dunias, Z. S., Van Calster, B., Timmerman, D., Boulesteix, A. L. & van Smeden, M. A comparison of hyperparameter tuning procedures for clinical prediction models: A simulation study. *Stat. Med.* **43**, 1119–1134. <https://doi.org/10.1002/sim.9932> (2024).

Acknowledgements

This research was funded by the EveryCat Health Foundation (CaPK22-002), by the Research Foundation – Flanders (FWO, FWO SBP 2020 006001) and by the Industrial Research Fund of Ghent University (IOF, F2021/IOF-Equip/014). The authors would like to express their gratitude to the owners of the cats that provided blood and urine samples, and to the veterinarians referring their patients to us to make this study possible. Additionally, they would like to extend their appreciation to Emmanuel Abatih for his assistance in the statistical processing of the data.

Author contributions

Funding acquisition and methodology were conducted by E.V.B., L.V.M., L.V and S.D. Supervision was performed by L.V. and S.D. Samples and metadata were collected by E.V.B. and L.V.M., followed by metabolomics analyses and data processing. Statistical analysis, data interpretation and visualization were performed by E.V.B. Manuscript writing was performed by E.V.B., and reviewing and editing by E.V.B., E.D.P., L.V., S.D. and D.P. All authors reviewed and approved the final manuscript.

Declarations

Competing interests

The authors declare no competing interests.

Additional information

Supplementary Information The online version contains supplementary material available at <https://doi.org/10.1038/s41598-025-90019-x>.

Correspondence and requests for materials should be addressed to L.V.

Reprints and permissions information is available at www.nature.com/reprints.

Publisher's note Springer Nature remains neutral with regard to jurisdictional claims in published maps and institutional affiliations.

Open Access This article is licensed under a Creative Commons Attribution-NonCommercial-NoDerivatives 4.0 International License, which permits any non-commercial use, sharing, distribution and reproduction in any medium or format, as long as you give appropriate credit to the original author(s) and the source, provide a link to the Creative Commons licence, and indicate if you modified the licensed material. You do not have permission under this licence to share adapted material derived from this article or parts of it. The images or other third party material in this article are included in the article's Creative Commons licence, unless indicated otherwise in a credit line to the material. If material is not included in the article's Creative Commons licence and your intended use is not permitted by statutory regulation or exceeds the permitted use, you will need to obtain permission directly from the copyright holder. To view a copy of this licence, visit <http://creativecommons.org/licenses/by-nc-nd/4.0/>.

© The Author(s) 2025